Elasto-plasticity of heterogeneous materials at different scales

Pierre Suquet, Noël Lahellec

Proceedings of the 23rd International Conference in Theoretical and Applied Mechanics. Beijing (China). August 19-24 2012.

Mechanics of polycrystalline and heterogeneous materials at different scales

P. Suquet [1,2a], N. Lahellec[2,1]

[1] CNRS. LMA. UPR 7051. 13402. Marseille Cedex 20. France.
[2]Aix-Marseille Université. 60 rue Frédéric Joliot-Curie, 13453 Marseille Cedex 13, France.

Abstract

Virtually every solid material contains features that are different at different length scales. The challenge, both for mathematical and physical modeling, is to comprehend relationships between models at different length scales. This has led to a well-developed theory of "homogenization" mostly concentrating on the prediction of the effective response of heterogeneous materials. However emerging characterization methods in Experimental Mechanics, giving access to local fields at smaller and smaller scales pose another challenge to modelers to devise efficient formulations that permit interpretation and exploitation of the massive amount of data generated by these novel methods. Significant progress has been made in the last twenty years to model nonlinear heterogeneous materials which are made either from purely elastic or purely dissipative constituents. Emphasis is put here on the coupling between elastic and plastic effects. Incremental variational principles are exploited to propose approximate mean-field methods to predict accurately the overall response of heterogeneous materials as well as some of the statistics of the local fields.

Keyword polycrystal / ice / creep / elastoviscoplasticity / numerical homogenization / Fourier transform.

1 Introduction

Virtually every solid material is heterogeneous at one, and often several, length scales. Identifying the main physical mechanisms at a given scale and

[a]suquet@lma.cnrs-mrs.fr

understanding how the interactions between these mechanisms result in a collective behavior at a larger scale has led to the development of several theories under a wide variety of names such as "up-scaling", "coarse-graining", "micromechanics" , "effective medium", "mean-field" or "homogenization" theories covering several decades of length-scales spanned by solid materials from the nano-scale to the laboratory scale. All these approaches may have differences, sometimes significant, in their perspectives to the problem, but they all aim at extracting the most pertinent information from the micro scale (the smaller scale) to the macro scale (the coarser scale). The present study is limited to scales ranging from micrometers to centimeters, where Continuum Mechanics applies and where the above mentioned approaches considering at least two different scales have made considerable progress in the past 20 years.

Progress are currently being made in three different, but intimately connected, directions:

- *New experimental techniques* at small scales are developed to provide information on the microstructure (see Uchic *et al* [1] for instance), on the local mechanisms and on the *in situ* constitutive relations of the phases at the micro scale.

- *New mean-field or homogenization theories*, delivering fast accurate estimates of the effective properties of materials and other pertinent information are proposed to deal from an engineering (macroscopic) perspective with structures which are heterogeneous at small scale and to incorporate enough information about their microscopic variability in the prediction of their macroscopic response (see Ponte Castañeda and Suquet [2] for instance).

- *Full-field simulations* at the volume element level, challenged by the progress in experimental techniques, are constantly improved to check the consistency of homogenization theories with experimental results, to provide information that are not accessible experimentally and to perform extensive and accurate parametric studies to calibrate models (see Lebensohn *et al* [3] for FFT-based approaches).

The present study will emphasize two specific aspects of micromechanical problems encountered in heterogeneous materials:

1. *Coupling between elastic and dissipative effects in heterogeneous materials.* New nonlinear homogenization theories have been developed in the last twenty years to model nonlinear heterogeneous materials which are made *either from purely elastic or purely dissipative constituents* (Willis [4], Ponte Castañeda [5], Ponte Castañeda and Suquet [2]). However, by contrast the question of the coupling between elastic and dissipative effects, which is, in practice, the rule rather than the exception, has not witnessed the same development.

2. *Importance of intraphase strain heterogeneity.* Emerging characterization methods in Experimental Mechanics, giving access to local fields at smaller and smaller scales have shown the multiscale character of deformation structures (Doumalin *et al* [6], Bourcier *et al* [7]). These finer experimental techniques pose a challenge to modelers to devise efficient formulations that permit interpretation and exploitation of the massive amount of data generated by these novel methods. It has become clear in the past decade that homogenization schemes could not be limited to predicting effective properties, or phase averages of the fields, but should also deliver more local information about their distribution and variability in the individual phases. Interestingly, Ponte Castañeda [8] has shown the importance of intraphase field fluctuations, in addition to field averages per phase, in the context of materials with a single type of deformation (elastic or viscous). In the somewhat different context of viscoelastic composites, Lahellec and Suquet [9] have also shown that it is necessary to transfer higher-order statistics of the fields from one time-step to the other. The purpose of the present study is to extend, at least partially, these results to elasto-(visco)plastic composites.

2 Motivation and orientation

2.1 Coupling elastic and plastic deformations

To illustrate the practical issues posed by the interaction between elasticity and plasticity, we describe two specific situations where it plays an important role.

1. *Bauschinger effect in heterogeneous materials.* A strong Bauschinger effect is commonly observed in metal-matrix composites (Corbin *et al*

[10]). This effect is illustrated in figure 1a where a typical stress-strain curve of a duplex steel subject to loading-unloading is shown (full-field simulations are due to Brassart *et al* [11])). After unloading, the yield stress in compression of the steel is seen to be much lower than the stress which was reached during the loading phase, just before unloading the specimen. One of the most advanced micromechanical model available to-date, the incremental mean-field approach of Doghri *et al* [12] using an isotropic tangent modulus for the matrix, underestimates significantly the kinematic hardening of the composite upon unloading, as can be seen in figure 13a of [12]. Capturing accurately the asymmetry between loading and unloading is, indeed, a challenge for all existing mean-field approaches.

To investigate this problem by means of a micromechanical approach, the constitutive relations of the individual constituents are required. Duplex steels are made of a ferritic (soft) phase reinforced by martensitic (hard) inclusions which can be considered as purely elastic. A good description of the stress-strain response of the matrix is provided by the following constitutive relations (for simplicity, only linear kinematic hardening is considered here).

$$\left.\begin{aligned} &\dot{\boldsymbol{\varepsilon}} = \boldsymbol{M} : \dot{\boldsymbol{\sigma}} + \dot{\boldsymbol{\varepsilon}}^{\mathsf{p}}, \quad \dot{\boldsymbol{\varepsilon}}^{\mathsf{p}} = \frac{3}{2}\dot{p}\frac{\boldsymbol{s}-\boldsymbol{X}}{(\sigma - X)_{\mathsf{eq}}}, \\ &\boldsymbol{X} = \boldsymbol{H} : \boldsymbol{\varepsilon}^{\mathsf{p}},\ \dot{p} = \dot{\varepsilon}_0 \left(\frac{[(\sigma - X)_{\mathsf{eq}} - \sigma_Y - R(p)]^+}{\eta} \right)^n . \end{aligned}\right\} \tag{1}$$

where $\boldsymbol{\varepsilon}$ is the linearized strain, $\boldsymbol{\sigma}$ is the Cauchy stress and $\boldsymbol{s}$ is the stress deviator, $\boldsymbol{M}$ is the elastic compliance of the material, $\boldsymbol{X}$ is the back stress, a (traceless) second-order tensor associated with kinematic hardening, $(\sigma - X)_{\mathsf{eq}} = \left(\frac{3}{2}(\boldsymbol{s}-\boldsymbol{X}) : (\boldsymbol{s}-\boldsymbol{X})\right)^{1/2}$ is the von Mises norm of $\boldsymbol{\sigma} - \boldsymbol{X}$, p is the accumulated plastic strain defined as $\dot{p} = \dot{\varepsilon}^{\mathsf{p}}_{\mathsf{eq}} = \left(\frac{2}{3}\dot{\boldsymbol{\varepsilon}}^{\mathsf{p}} : \dot{\boldsymbol{\varepsilon}}^{\mathsf{p}}\right)^{1/2}$, $R(p)$ is a nonnegative scalar parameter associated with isotropic hardening, n is the rate-sensitivity exponent. Rate-independent plasticity (with isotropic and kinematic hardening) is obtained in the limit as n tends to $+\infty$.

2. *Transient (or primary) creep in polycrystalline materials.* Another problem where both elastic and plastic strains are intimately coupled is primary creep in polycrystalline materials. A typical experimental

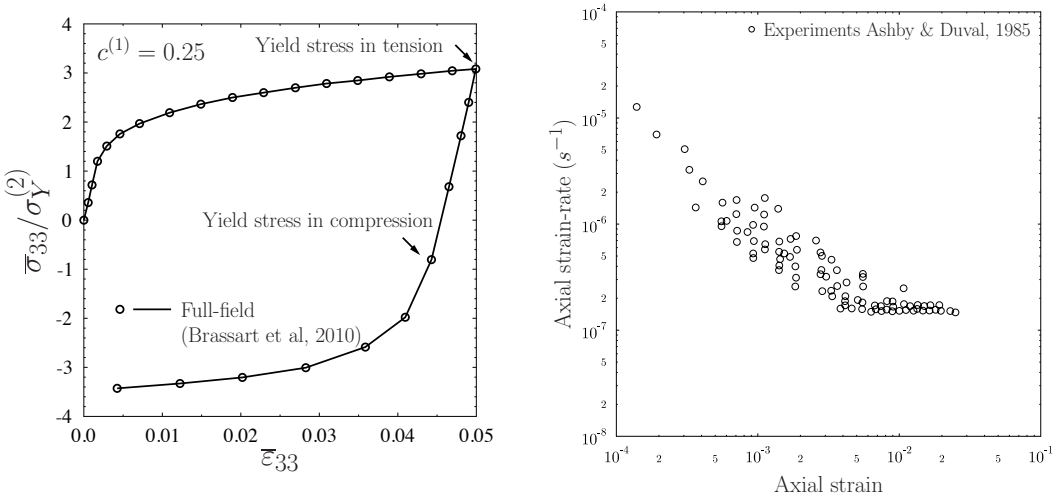

Figure 1: Two examples of problems arising from the coupling between elastic and plastic deformations in heterogeneous materials. (a): Bauschinger effect in dual-phase steels. After Brassart *et al* [11] and Doghri *et al* [12]. (b): Transient creep experiments on polycrystalline ice at -10^0C. Experimental results compiled by Ashby and Duval [13].

creep curve compiled by Ashby and Duval [13] for polycrystalline ice is shown in figure 1b. The strain rate is seen to undergo a transition from its instantaneous response (immediately after the application of the stress) where elastic effects are dominant, to a stationary regime (secondary creep) determined only by the viscous properties of the polycrystal.

Constitutive relations for ice at the single crystal level have been proposed by Castelnau *et al* [14] and subsequently modified by Suquet *et al* [15]:

$$\left.\begin{array}{c} \boldsymbol{\varepsilon} = \boldsymbol{\varepsilon}^{\mathsf{e}} + \boldsymbol{\varepsilon}^{\mathsf{vp}}, \quad \boldsymbol{\varepsilon}^{\mathsf{e}} = \boldsymbol{M} : \boldsymbol{\sigma}, \quad \boldsymbol{\varepsilon}^{\mathsf{vp}} = \displaystyle\sum_{k=1}^{M} \gamma_k \boldsymbol{\mu}_k, \quad \boldsymbol{\mu}_k = \boldsymbol{m}_k \otimes_s \boldsymbol{n}_k, \\ \dot{\gamma}_k = \dot{\gamma}_{0,k} \left(\dfrac{|\tau_k - X_k|}{\tau_{0,k}} \right)^{n_k} \operatorname{sgn}(\tau_k - X_k), \\ \dot{\tau}_{0,k} = (\tau_{sta,k} - \tau_{0,k})\, \dot{p}_k, \quad \dot{p}_k = \displaystyle\sum_{\ell=1}^{M} h_{k\ell} \ |\dot{\gamma}_\ell|, \\ \dot{X}_k = c_k \dot{\gamma}_k - d_k X_k |\dot{\gamma}_k| - e_k X_k. \end{array}\right\} \quad (2)$$

Polycrystalline ice is an aggregate of grains obeying the same constitutive relations (2) but with different orientations. After rotation, and because of the anisotropy of the single crystal, the elastic compliance $\boldsymbol{M}$ and the slip systems $\boldsymbol{\mu}_k$ differ from one grain to the other in a fixed frame and each grain has to be considered as a different phase in a large aggregate. A polycrystal is therefore a composite material with many phases.

2.2 Effective relations, averages and field fluctuations

Micromechanics relies on the analysis of a *representative volume element (r.v.e.)*. Such a volume V is comprised of N phases occupying domains $V^{(r)}$ with characteristic functions $\chi^{(r)}$ and volume fraction $c^{(r)}$ and must be large enough to contain most of the available statistical information on the microstructure of the composite. The spatial averages over the whole volume element V and over the phases $V^{(r)}$ are denoted by $\langle . \rangle$ and $\langle . \rangle^{(r)}$ respectively. The average (or first moment) of the stress and strain field over the whole volume element and over phase r are respectively denoted as :

$$\overline{\boldsymbol{\sigma}} = \langle \boldsymbol{\sigma} \rangle = \frac{1}{|V|} \int_V \boldsymbol{\sigma}(\boldsymbol{x}) \ d\boldsymbol{x}, \quad \overline{\boldsymbol{\sigma}}^{(r)} = \langle \boldsymbol{\sigma} \rangle^{(r)} = \frac{1}{|V^{(r)}|} \int_{V^{(r)}} \boldsymbol{\sigma}(\boldsymbol{x}) \ d\boldsymbol{x}, \quad (3)$$

with similar definitions for the averages of the strain. Effective properties of a composite are defined as the relation between the history (in time) of the average stress $\overline{\boldsymbol{\sigma}}(t), 0 \leq t \leq T$ and the history of average strain $\overline{\boldsymbol{\varepsilon}}, 0 \leq t \leq T$. The history of one of the two averages is prescribed and the other is deduced from the corresponding local field by the averaging relations (3). In full generality, the determination of the effective constitutive relations of the composite require the local fields $\boldsymbol{\sigma}(\boldsymbol{x})$ and $\boldsymbol{\varepsilon}(\boldsymbol{x})$ to be determined by solving the compatibility equations, the equilibrium equations and the constitutive relations for the individual phases. This is indeed a formidable problem and very few exact solutions are known.

The situation simplifies significantly when the individual phases are linear elastic. Denoting by $\boldsymbol{L}^{(r)}$ the elastic moduli in phase r, the effective stiffness of the composite is completely specified as soon as only *the average strain* $\overline{\boldsymbol{\varepsilon}}^{(r)}$ *in each individual phase is known* in terms of the total average strain $\overline{\boldsymbol{\varepsilon}}$. Since the problem is linear, this relation can be expressed as $\overline{\boldsymbol{\varepsilon}}^{(r)} = \boldsymbol{A}^{(r)} : \overline{\boldsymbol{\varepsilon}}$ and the effective stiffness $\widetilde{\boldsymbol{L}}$ of the composite reads as:

$$\overline{\boldsymbol{\sigma}} = \widetilde{\boldsymbol{L}} : \overline{\boldsymbol{\varepsilon}}, \quad \widetilde{\boldsymbol{L}} = \sum_{r=1}^{N} c^{(r)} \boldsymbol{L}^{(r)} : \boldsymbol{A}^{(r)}.$$

The complete knowledge of the local field $\boldsymbol{\varepsilon}(\boldsymbol{x})$ is not required. This result, which again is *exact* for linear composites, partly explains why little attention has been paid in the literature to the fluctuations of the fields within individual phases (hereafter called *intraphase field fluctuations* after Ponte Castañeda [8]).

When the phases are nonlinear, field fluctuations play an important role. Assuming for instance that the stress-strain relations are hyperelastic in the form $\boldsymbol{\sigma}(\boldsymbol{x}) = \mathcal{F}^{(r)}(\boldsymbol{\varepsilon}(\boldsymbol{x}))$, the strain field can be expanded about its mean-value (following Ponte Castañeda [16]):

$$\boldsymbol{\varepsilon}(\boldsymbol{x}) = \overline{\boldsymbol{\varepsilon}}^{(r)} + (\boldsymbol{\varepsilon}(\boldsymbol{x}) - \overline{\boldsymbol{\varepsilon}}^{(r)}),$$

and the corresponding Taylor expansion for the stress reads as:

$$\begin{aligned} \boldsymbol{\sigma}(\boldsymbol{x}) &= \mathcal{F}^{(r)}(\overline{\boldsymbol{\varepsilon}}^{(r)}) + \frac{\partial \mathcal{F}^{(r)}}{\partial \boldsymbol{\varepsilon}}(\overline{\boldsymbol{\varepsilon}}^{(r)}) : (\boldsymbol{\varepsilon}(\boldsymbol{x}) - \overline{\boldsymbol{\varepsilon}}^{(r)}) \\ &+ \frac{1}{2}\frac{\partial^2 \mathcal{F}^{(r)}}{\partial^2 \boldsymbol{\varepsilon}}(\overline{\boldsymbol{\varepsilon}}^{(r)}) : (\boldsymbol{\varepsilon}(\boldsymbol{x}) - \overline{\boldsymbol{\varepsilon}}^{(r)}) \otimes (\boldsymbol{\varepsilon}(\boldsymbol{x}) - \overline{\boldsymbol{\varepsilon}}^{(r)}) + ... \end{aligned}$$

It is readily seen that

$$\overline{\boldsymbol{\sigma}} = \sum_{r=1}^{N} c^{(r)} \overline{\boldsymbol{\sigma}}^{(r)}$$

$$\text{with} \quad \overline{\boldsymbol{\sigma}}^{(r)} = \mathcal{F}^{(r)}(\overline{\boldsymbol{\varepsilon}}^{(r)}) + \frac{1}{2}\frac{\partial^2 \mathcal{F}^{(r)}}{\partial^2 \boldsymbol{\varepsilon}}(\overline{\boldsymbol{\varepsilon}}^{(r)}) : \left\langle (\boldsymbol{\varepsilon} - \overline{\boldsymbol{\varepsilon}}^{(r)}) \otimes (\boldsymbol{\varepsilon} - \overline{\boldsymbol{\varepsilon}}^{(r)}) \right\rangle^{(r)} + ...$$

Therefore the fluctuations of the strain field in phase r contribute directly to the average stress $\overline{\boldsymbol{\sigma}}$. Fluctuations of the fields do matter in nonlinear composites.

Another possible origin to the relative lack of interest for higher-order statistics of the fields in the context of polycrystalline materials, is a common misinterpretation of the landmark paper by Eshelby [17]. Eshelby shows that the strain $\boldsymbol{\varepsilon}^{(I)}$ within an ellipsoidal elastic inclusion in an infinite medium of different elastic characteristics, subjected to an applied deformation $\overline{\boldsymbol{\varepsilon}}$ at infinity, is uniform in the inclusion. Some of the earliest versions of the self-consistent scheme took advantage of this exact result to derive an estimate for the effective properties of polycrystals by considering each grain (or each family of grains sharing the same shape and the same crystallographic orientation) as a single ellipsoidal inclusion in a surrounding infinite homogeneous medium. According to Eshelby's result, the stress and strain are uniform in the inclusion (and therefore in each grain) in this self-consistent vision of a polycrystal. Extending this "result" from elastic to elasto-plastic polycrystals by considering tangent elastoplastic moduli, this interpretation by the self-consistent scheme has led to the incorrect belief that the stress and strain are uniform in individual grains of an elasto-plastic polycrystal, leading to mean-field approaches based only on the first moments of the stress or strain fields. The uniformity of the strain field within each grain is clearly contradicted by experimental observations and by numerical simulations.

2.3 Field heterogeneity

Strain fields are observed both experimentally and numerically to be highly heterogeneous, as shown in figure 2. The figure on the left shows a map of the equivalent strain field measured by digital image correlation (Doumalin *et al* [6]). The grain boundaries are shown in white and it is clear that the strain field is heterogeneous within the same grain. Rather than being uniform in each grain, the main feature of the strain field is the formation of

bands running at $\pm 45^0$ from the tensile direction (vertical) and crossing the grains with local deviations depending on whether a grain is well oriented or not. The same trends are observed in full-field simulations. For instance, figure 2 right shows a snapshot of the equivalent strain in an aggregate of polycrystalline ice after 40 h of creep and again the strain is not uniform in each grain. The bias in the application of Eshelby's result to polycrystals was pointed out by Hashin [18]: *"the self-consistent scheme assumes that a tree sees the forest - but a tree sees only other trees"*. In other words, grain-to-grain interactions are essential in understanding the structure of the strain (or stress) field in polycrystals.

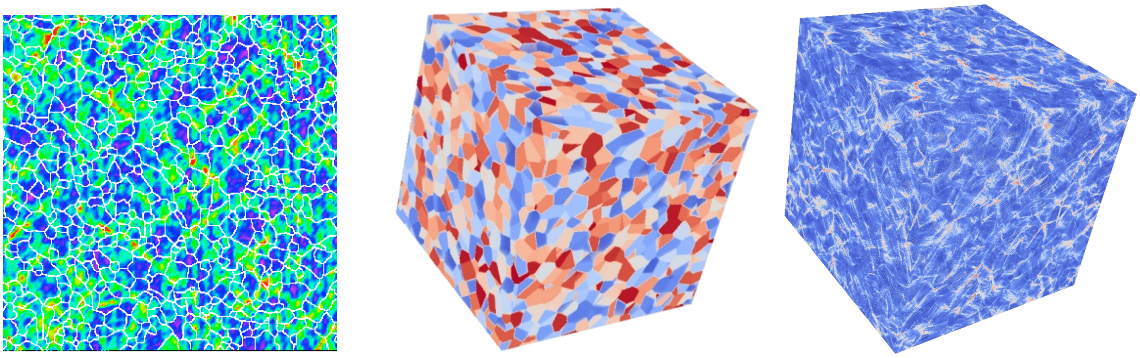

Figure 2: Field heterogeneity. Left: Map of the equivalent deformation (obtained by DIC) in a Zirconium polycrystal subjected to a tensile test in the vertical direction. Grain boundaries are shown in white (courtesy of M. Bornert). Center and right: Full-field simulation of a creep test on polycrystalline ice. Center: microstructure. Right: snapshot of the equivalent deformation after 40h of creep under an applied vertical stress of 1 MPa.

The present study highlights the fact that accurate micromechanical theories should take into account *"higher-order statistics of the fields"*. Higher-order statistics is limited here to first and second-order moments per phase of the fields. For the strain field, these moments are $\overline{\boldsymbol{\varepsilon}}^{(r)} = \langle \boldsymbol{\varepsilon} \rangle^{(r)}$ and $\langle \boldsymbol{\varepsilon} \otimes \boldsymbol{\varepsilon} \rangle^{(r)}$, or equivalently the average strain $\overline{\boldsymbol{\varepsilon}}^{(r)}$ and the fourth-order tensor of the strain fluctuations $\boldsymbol{C}^{(r)}(\boldsymbol{\varepsilon})$ defined as:

$$\boldsymbol{C}^{(r)}(\boldsymbol{\varepsilon}) = \frac{1}{2} \big\langle (\boldsymbol{\varepsilon} - \overline{\boldsymbol{\varepsilon}}^{(r)}) \otimes (\boldsymbol{\varepsilon} - \overline{\boldsymbol{\varepsilon}}^{(r)}) \big\rangle^{(r)}.$$

It is now well-known ([2, 19, 20]) that these moments can be computed ex-

actly for thermoelastic composites from the effective properties of the composite. Assume that the phases are linearly thermoelastic, with constitutive relations:

$$\boldsymbol{\sigma}(\boldsymbol{x}) = \boldsymbol{L}^{(r)} : \boldsymbol{\varepsilon}(\boldsymbol{x}) + \boldsymbol{\tau}^{(r)} \quad \text{in phase } r, \tag{4}$$

where $\boldsymbol{L}^{(r)}$ and $\boldsymbol{\tau}^{(r)}$ are uniform in phase r and define the free-energy of phase r as

$$w^{(r)}(\boldsymbol{L}^{(r)}, \boldsymbol{\tau}^{(r)}, \boldsymbol{\varepsilon}) = \frac{1}{2}\boldsymbol{\varepsilon} : \boldsymbol{L}^{(r)} : \boldsymbol{\varepsilon} + \boldsymbol{\tau}^{(r)} : \boldsymbol{\varepsilon}.$$

Then the first and second moments of the strain field in phase r are given by

$$\langle \boldsymbol{\varepsilon} \rangle^{(r)} = \frac{1}{c^{(r)}} \frac{\partial \widetilde{w}}{\partial \boldsymbol{\tau}^{(r)}}, \quad \langle \boldsymbol{\varepsilon} \otimes \boldsymbol{\varepsilon} \rangle^{(r)} = \frac{2}{c^{(r)}} \frac{\partial \widetilde{w}}{\partial \boldsymbol{L}^{(r)}}. \tag{5}$$

where $\widetilde{w}$ is the effective free-energy of the composite. The corresponding statistics of the stress field follow from (5) and (4):

$$\langle \boldsymbol{\sigma} \rangle^{(r)} = \boldsymbol{L}^{(r)} : \langle \boldsymbol{\varepsilon} \rangle^{(r)} + \boldsymbol{\tau}^{(r)}, \quad \boldsymbol{C}^{(r)}(\boldsymbol{\sigma}) = \boldsymbol{C}^{(r)}(\boldsymbol{L}^{(r)} : \boldsymbol{\varepsilon}). \tag{6}$$

2.4 Accounting for the material history: lessons from linear viscoelastic composites

The problem at hand, when dealing with elasto-(visco)plastic materials, is an evolution problem in time. The history dependence of the constitutive relations raises the question of *which information about the fields (stress, strain) should be transferred from one time-step to the next by a mean-field approach?* If the local fields are fully resolved in full-field approaches, it is not the case in mean-field approaches. Lessons can be learnt from linear viscoelastic composites.

Linear viscoelastic composites appear naturally in the problem of elasto-(visco)plastic composites for two reasons. First, they correspond to a particular case of the constitutive relations (1) (no yield stress, no hardening, rate-sensitivity exponent $n = 1$). Second, the linearization of the constitutive relations, which is a common practice when the constituents are either purely hyperelastic or purely viscous, leads naturally to linear viscoelastic composites when the constituents are elasto-viscoplastic. Although the effective response of linear viscoelastic composites is relatively well understood, thanks to the Laplace transform which permits to translate the problem for a linear viscoelastic composite into a problem for a linear elastic composite,

the question of determining the second moments of the stress field in the individual phases of a viscoelastic composite has not yet received a satisfactory answer. Without these second moments, most "modern" linearization methods outlined in the sequel cannot be applied.

A way around this problem is, instead of using the Laplace transform, to discretize in time the evolution equations for a viscoelastic composite which read as

$$\dot{\boldsymbol{\varepsilon}}(\boldsymbol{x},t) = \boldsymbol{M}^{(r)} : \dot{\boldsymbol{\sigma}}(\boldsymbol{x},t) + \boldsymbol{M}^{\mathsf{v}(r)} : \boldsymbol{\sigma}(\boldsymbol{x},t) \quad \text{in phase } r,$$

where $\boldsymbol{M}^{\mathsf{v}(r)}$ is the viscosity tensor of phase r. After time-discretization, using a backward differentiation scheme $\dot{f}(t_{n+1}) \simeq \frac{f_{n+1}-f_n}{\Delta t}$ (where f_n denotes $f(t_n)$), the constitutive equations read as

$$\dot{\boldsymbol{\varepsilon}}_{n+1}(\boldsymbol{x}) = \left(\frac{1}{\Delta t}\boldsymbol{M}^{(r)} + \boldsymbol{M}^{\mathsf{v}(r)}\right) : \boldsymbol{\sigma}_{n+1}(\boldsymbol{x}) - \frac{1}{\Delta t}\boldsymbol{M}^{(r)} : \boldsymbol{\sigma}_n(\boldsymbol{x}) \quad \text{in phase } r. \tag{7}$$

The constitutive relations for a viscoelastic composite correspond, after time-discretization, to *a nonclassical thermoelastic problem* with piecewise uniform elastic compliance $\frac{1}{\Delta t}\boldsymbol{M}^{(r)} + \boldsymbol{M}^{\mathsf{v}(r)}$ but with *a nonuniform eigenstrain* $-\frac{1}{\Delta t}\boldsymbol{M}^{(r)} : \boldsymbol{\sigma}_n(\boldsymbol{x})$. Second moments of the stress field in such nonclassical thermoelastic composites are not known. However, when the nonuniform field $\boldsymbol{\sigma}_n(\boldsymbol{x})$ can be approximated by a uniform stress $\boldsymbol{\sigma}_n^{(r)}$ in each individual phase r, these second moments are known. The aim of the present work is precisely to approximate (in a variational sense) the problem (7) by a problem where the eigenstrain is piecewise uniform. A similar problem was addressed in [21].

In a first attempt, the stress field $\boldsymbol{\sigma}_n(\boldsymbol{x})$ can be replaced in each phase by its average over this phase:

$$\boldsymbol{\sigma}_n(\boldsymbol{x}) \simeq \overline{\boldsymbol{\sigma}}_n^{(r)} = \langle \boldsymbol{\sigma}_n \rangle^{(r)} \quad \text{in phase } r. \tag{8}$$

This approximation is a *first moment* approximation. Unfortunately this simple model is rather inaccurate, as discussed by Lahellec and Suquet [22] for linear viscoelastic composites. In order to get satisfactory results, it is indeed necessary to account for the second moment of $\boldsymbol{\sigma}_n$ in each phase (in addition to the first moment) in the definition of $\boldsymbol{\sigma}_n^{(r)}$ ([22]).

The orientation of this paper is as follows:

1. Establish variational principles governing the evolution of nonlinear elasto-viscoplastic composites.

2. Adapt the variational method of Ponte Castañeda [23] to these variational principles, both for the linearization of the constitutive relations and for the approximation of the stress field from the previous time step by a piecewise uniform stress.

3 Variational Principles for elasto-(visco)-plastic composites

3.1 Individual constituents

The constitutive relations (1) can be formulated in the framework of *Generalized Standard Materials* with two convex potentials. The first potential is the free-energy density $w(\boldsymbol{\varepsilon}, \boldsymbol{\alpha})$ which depends on the (infinitesimal) strain $\boldsymbol{\varepsilon}$ and on *internal* variables $\boldsymbol{\alpha}$ describing irreversible phenomena. The stress $\boldsymbol{\sigma}$ and the driving forces $\boldsymbol{\mathcal{A}}$ triggering the evolution of the internal variables $\boldsymbol{\alpha}$ derive from the free-energy density w through:

$$\boldsymbol{\sigma} = \frac{\partial w}{\partial \boldsymbol{\varepsilon}}(\boldsymbol{\varepsilon}, \boldsymbol{\alpha}), \quad \boldsymbol{\mathcal{A}} = -\frac{\partial w}{\partial \boldsymbol{\alpha}}(\boldsymbol{\varepsilon}, \boldsymbol{\alpha}). \tag{9}$$

The evolution of the internal variables $\boldsymbol{\alpha}$ is governed by the driving forces $\boldsymbol{\mathcal{A}}$ according to

$$\boldsymbol{\mathcal{A}} = \frac{\partial \varphi}{\partial \dot{\boldsymbol{\alpha}}}(\dot{\boldsymbol{\alpha}}), \quad \text{or equivalently} \quad \dot{\boldsymbol{\alpha}} = \frac{\partial \varphi^*}{\partial \boldsymbol{\mathcal{A}}}(\boldsymbol{\mathcal{A}}), \tag{10}$$

where the dissipation potential $\varphi(\dot{\boldsymbol{\alpha}})$ is the second potential defining the model and φ^* denotes its Legendre transform. Upon elimination of $\boldsymbol{\mathcal{A}}$ between (9) and (10), the constitutive relations of the materials under consideration can be re-written as a system of two coupled equations, one of them being a differential equation in time for $\boldsymbol{\alpha}$:

$$\boldsymbol{\sigma} = \frac{\partial w}{\partial \boldsymbol{\varepsilon}}(\boldsymbol{\varepsilon}, \boldsymbol{\alpha}), \quad \frac{\partial w}{\partial \boldsymbol{\alpha}}(\boldsymbol{\varepsilon}, \boldsymbol{\alpha}) + \frac{\partial \varphi}{\partial \dot{\boldsymbol{\alpha}}}(\dot{\boldsymbol{\alpha}}) = 0. \tag{11}$$

For instance in the case of the constitutive relations (1) the internal variables are $\boldsymbol{\alpha} = (\boldsymbol{\varepsilon}^{\mathsf{p}}, p)$ and the two potentials read as

$$\left.\begin{array}{c} w(\boldsymbol{\varepsilon}, \boldsymbol{\alpha}) = \frac{1}{2}\,(\boldsymbol{\varepsilon} - \boldsymbol{\varepsilon}^{\mathsf{p}}) : \boldsymbol{L} : (\boldsymbol{\varepsilon} - \boldsymbol{\varepsilon}^{\mathsf{p}}) + w_{st}(p) + \frac{1}{2}\boldsymbol{\varepsilon}^{\mathsf{p}} : \boldsymbol{H} : \boldsymbol{\varepsilon}^{\mathsf{p}}, \\ w_{st}(p) = \int_0^p R(q)dq, \end{array}\right\} \tag{12}$$

and

$$\varphi(\dot{\boldsymbol{\alpha}}) = \sigma_Y \dot{\varepsilon}^{\mathsf{p}}_{\mathsf{eq}} + \frac{\eta \dot{\varepsilon}_0}{m+1}\left(\frac{\dot{\varepsilon}^{\mathsf{p}}_{\mathsf{eq}}}{\dot{\varepsilon}_0}\right)^{m+1}. \tag{13}$$

The time derivative $\dot{\boldsymbol{\alpha}}$ in (11) can be approximated by a difference quotient after use of an implicit (backward) Euler-scheme known for its stability and consistence. The time interval of study $[0, T]$ is discretized into time intervals $t_0 = 0, t_1, ..., t_n, t_{n+1}, ..., t_N = T$. For simplicity the time step $t_{n+1} - t_n$ is denoted by Δt (its dependence on n is omitted for simplicity) and the value $f(t_n)$ of a function f evaluated at time t_n is denoted by f_n. Assuming that $(\boldsymbol{\varepsilon}_n, \boldsymbol{\alpha}_n)$ are known at time t_n, the time-discretization procedure applied to (11) leads to the discretized system for the unknowns $(\boldsymbol{\varepsilon}_{n+1}, \boldsymbol{\alpha}_{n+1})$:

$$\boldsymbol{\sigma}_{n+1} = \frac{\partial w}{\partial \boldsymbol{\varepsilon}}(\boldsymbol{\varepsilon}_{n+1}, \boldsymbol{\alpha}_{n+1}), \quad \frac{\partial w}{\partial \boldsymbol{\alpha}}(\boldsymbol{\varepsilon}_{n+1}, \boldsymbol{\alpha}_{n+1}) + \frac{\partial \varphi}{\partial \dot{\boldsymbol{\alpha}}}\left(\frac{\boldsymbol{\alpha}_{n+1} - \boldsymbol{\alpha}_n}{\Delta t}\right) = 0. \tag{14}$$

3.2 Variational principles for single constituents

When the two potentials w and φ are convex, variational principles governing the evolution of generalized standard materials have been used for a long time (see for instance Mialon [24]). They have recently been extended to nonconvex potentials and have found a new domain of applications with the prediction of microstructure formation (Ortiz and Repetto [25], Miehe *et al* [26]). The variational principles used in the present study are limited to *convex* potentials.

Lahellec and Suquet ([9] and [27] have derived two variational principles whose Euler-Lagrange equations are the relations (14).

1. *Total (or Incremental) Variational Principle.* Considering $(\boldsymbol{\varepsilon}_{n+1}, \boldsymbol{\alpha}_{n+1})$, the strain and internal variables at the end of the time-step as the main unknowns, it is observed that the second equation in (14) is the Euler-Lagrange equation for the variational problem:

$$\inf_{\boldsymbol{\alpha}} \quad J(\boldsymbol{\varepsilon}_{n+1}, \boldsymbol{\alpha}), \quad J(\boldsymbol{\varepsilon}, \boldsymbol{\alpha}) = w(\boldsymbol{\varepsilon}, \boldsymbol{\alpha}) \; + \; \Delta t \; \varphi\left(\frac{\boldsymbol{\alpha} - \boldsymbol{\alpha}_n}{\Delta t}\right), \tag{15}$$

whereas the stress at the end of time-step is given as :

$$\boldsymbol{\sigma}_{n+1} = \frac{\partial w_\Delta}{\partial \boldsymbol{\varepsilon}}(\boldsymbol{\varepsilon}_{n+1}), \quad w_\Delta(\boldsymbol{\varepsilon}) = \inf_{\boldsymbol{\alpha}} \quad J(\boldsymbol{\varepsilon}, \boldsymbol{\alpha}). \tag{16}$$

The relation (16) between $\boldsymbol{\sigma}_{n+1}$ and $\boldsymbol{\varepsilon}_{n+1}$ can be seen as a generalized *nonlinear hyperelastic constitutive relation.*

2. *Rate Variational Principle.* Another variational principle can be derived when the variations are taken with respect to the rates $(\dot{\boldsymbol{\varepsilon}}, \dot{\boldsymbol{\alpha}})$ between t_n and t_{n+1}. Writing $\boldsymbol{\varepsilon}_{n+1}$ and $\boldsymbol{\alpha}_{n+1}$ as

$$\boldsymbol{\varepsilon}_{n+1} = \boldsymbol{\varepsilon}_n + \Delta t\ \dot{\boldsymbol{\varepsilon}}, \quad \boldsymbol{\alpha}_{n+1} = \boldsymbol{\alpha}_n + \Delta t\ \dot{\boldsymbol{\alpha}},$$

it is readily seen that the second equation in (14) is the Euler-Lagrange equation for the variational problem :

$$\inf_{\dot{\boldsymbol{\alpha}}} \quad \mathcal{D}(\dot{\boldsymbol{\varepsilon}}, \dot{\boldsymbol{\alpha}}),$$

$$\mathcal{D}(\dot{\boldsymbol{\varepsilon}}, \dot{\boldsymbol{\alpha}}) = \frac{1}{\Delta t}\left[w(\boldsymbol{\varepsilon}_n + \Delta t\ \dot{\boldsymbol{\varepsilon}}, \boldsymbol{\alpha}_n + \Delta t\ \dot{\boldsymbol{\alpha}}) - w(\boldsymbol{\varepsilon}_n, \boldsymbol{\alpha}_n)\right] + \varphi\left(\dot{\boldsymbol{\alpha}}\right).$$

Furthermore

$$\boldsymbol{\sigma}_{n+1} = \frac{\partial d}{\partial \dot{\boldsymbol{\varepsilon}}}(\dot{\boldsymbol{\varepsilon}}), \quad \text{where} \quad d(\dot{\boldsymbol{\varepsilon}}) = \inf_{\dot{\boldsymbol{\alpha}}} \quad \mathcal{D}(\dot{\boldsymbol{\varepsilon}}, \dot{\boldsymbol{\alpha}}). \tag{17}$$

The relation (17) between $\boldsymbol{\sigma}_{n+1}$ and $\dot{\boldsymbol{\varepsilon}}$ can be seen as a generalized *nonlinear viscous constitutive relation.*

3.3 Application to composite materials

A representative volume element (r.v.e.) V of the composite is composed of N phases. Each individual phase is governed by the differential equations (11) with potentials $w^{(r)}$ and $\varphi^{(r)}$. The rate-potential $\mathcal{D}$ at a material point $\boldsymbol{x}$ in phase r reads as

$$\mathcal{D}(\dot{\boldsymbol{\varepsilon}}, \dot{\boldsymbol{\alpha}}, \boldsymbol{x}) = \frac{1}{\Delta t}\left[w^{(r)}(\boldsymbol{\varepsilon}_n(\boldsymbol{x}) + \Delta t\ \dot{\boldsymbol{\varepsilon}}, \boldsymbol{\alpha}_n(\boldsymbol{x}) + \Delta t\ \dot{\boldsymbol{\alpha}}) - w^{(r)}(\boldsymbol{\varepsilon}_n(\boldsymbol{x}), \boldsymbol{\alpha}_n(\boldsymbol{x}))\right] + \varphi^{(r)}\left(\dot{\boldsymbol{\alpha}}\right)$$

with a similar definition for $J(\boldsymbol{\varepsilon}, \boldsymbol{\alpha}, \boldsymbol{x})$. It is essential to note that *the spatial dependence of $\mathcal{D}$ not only comes from the dependence of the potentials $w^{(r)}$*

and $\varphi^{(r)}$ on the phase, but also from the fields $\boldsymbol{\varepsilon}_n(\boldsymbol{x})$ and $\boldsymbol{\alpha}_n(\boldsymbol{x})$ from the previous time-step. Adopting the characterization (17)[b] of the stress $\boldsymbol{\sigma}_{n+1}$, the macroscopic stress $\overline{\boldsymbol{\sigma}}_{n+1} = \langle \boldsymbol{\sigma}_{n+1} \rangle$ can be characterized by the variational property:

$$\overline{\boldsymbol{\sigma}}_{n+1} = \frac{\partial \widetilde{d}}{\partial \dot{\overline{\boldsymbol{\varepsilon}}}} \left(\dot{\overline{\boldsymbol{\varepsilon}}} \right), \text{ where } \widetilde{d} \left(\dot{\overline{\boldsymbol{\varepsilon}}} \right) = \inf_{\langle \dot{\boldsymbol{\varepsilon}} \rangle = \dot{\overline{\boldsymbol{\varepsilon}}}} \langle d(\dot{\boldsymbol{\varepsilon}}) \rangle = \inf_{\langle \dot{\boldsymbol{\varepsilon}} \rangle = \dot{\overline{\boldsymbol{\varepsilon}}}} \left\langle \inf_{\dot{\boldsymbol{\alpha}}} \quad \mathcal{D}(\dot{\boldsymbol{\varepsilon}}, \dot{\boldsymbol{\alpha}}) \right\rangle. \quad (18)$$

The last variational problem in (18) is a difficult one as the potentials $w^{(r)}$ and $\varphi^{(r)}$ are non quadratic. Inspired by the variational method of Ponte Castañeda [23], the variational problem (18) is replaced by a simpler one for a potential $\mathcal{D}_0$ which will be specified in due time. $\mathcal{D}$ is written as:

$$\mathcal{D}(\dot{\boldsymbol{\varepsilon}}, \dot{\boldsymbol{\alpha}}) = \mathcal{D}_0(\dot{\boldsymbol{\varepsilon}}, \dot{\boldsymbol{\alpha}}) + \Delta\mathcal{D}(\dot{\boldsymbol{\varepsilon}}, \dot{\boldsymbol{\alpha}}), \quad \Delta\mathcal{D} = \mathcal{D} - \mathcal{D}_0, \quad (19)$$

where $\mathcal{D}_0(\dot{\boldsymbol{\varepsilon}}, \dot{\boldsymbol{\alpha}})$ is the rate-potential for a (fictitious) comparison composite which will be chosen in such a way that the comparison composite is indeed a *linear comparison composite (LCC)*. Using this translation, and optimizing over the LCC, the following estimate is obtained:

$$\left.\begin{aligned} \widetilde{d}(\dot{\overline{\boldsymbol{\varepsilon}}}) \simeq \operatorname*{Stat}_{\mathcal{D}_0} \quad & \left[\widetilde{d}_0(\dot{\overline{\boldsymbol{\varepsilon}}}) + \left\langle \operatorname*{Stat}_{\dot{\boldsymbol{\alpha}}, \dot{\boldsymbol{\varepsilon}}} \quad \Delta\mathcal{D}(\dot{\boldsymbol{\varepsilon}}, \dot{\boldsymbol{\alpha}}) \right\rangle \right], \\ \text{where} \quad & \widetilde{d}_0(\dot{\overline{\boldsymbol{\varepsilon}}}) = \inf_{\langle \dot{\boldsymbol{\varepsilon}} \rangle = \dot{\overline{\boldsymbol{\varepsilon}}}} \quad \left\langle \inf_{\dot{\boldsymbol{\alpha}}} \quad \mathcal{D}_0(\dot{\boldsymbol{\varepsilon}}, \dot{\boldsymbol{\alpha}}) \right\rangle \end{aligned} \right\} \quad (20)$$

The choice of $\mathcal{D}_0$ depends on the constitutive relations of the individual constituents.

3.4 Elasto-(visco)plastic phases with isotropic hardening

In the sample case of elasto-viscoplastic phases with isotropic hardening only ($\boldsymbol{X} = 0$ in (1)), the rate-potential reads as:

$$\begin{aligned} \mathcal{D}\left(\dot{\boldsymbol{\varepsilon}}, \dot{\boldsymbol{\varepsilon}}^{\mathsf{p}}, \dot{p}, \boldsymbol{x}\right) &= \frac{\Delta t}{2} \left[(\dot{\boldsymbol{\varepsilon}} - \dot{\boldsymbol{\varepsilon}}^{\mathsf{p}}) : \boldsymbol{L}^{(r)} : (\dot{\boldsymbol{\varepsilon}} - \dot{\boldsymbol{\varepsilon}}^{\mathsf{p}}) \right] + \boldsymbol{\sigma}_n(\boldsymbol{x}) : (\dot{\boldsymbol{\varepsilon}} - \dot{\boldsymbol{\varepsilon}}^{\mathsf{p}}) \\ &+ \frac{1}{\Delta t} \left(w_{st}^{(r)}(p_n(\boldsymbol{x}) + \Delta t \dot{p}) - w_{st}^{(r)}(p_n(\boldsymbol{x})) \right) \\ &+ \frac{\eta^{(r)} \dot{\varepsilon}_0}{m+1} \left(\frac{\dot{p}}{\dot{\varepsilon}_0} \right)^{m+1} + I_{\{\dot{p} = \dot{\varepsilon}^{\mathsf{p}}_{\mathsf{eq}}\}}(\dot{\boldsymbol{\alpha}}) \end{aligned}$$

[b] The reader is referred to Lahellec and Suquet [28] for the first approach based on the potential J.

where the indicator function $I_{\{\dot{p} = \dot{\varepsilon}^{\mathsf{p}}_{\mathsf{eq}}\}}$ enforces the constraint $\dot{p} = \dot{\varepsilon}^{\mathsf{p}}_{\mathsf{eq}}$. Note that $\mathcal{D}$ depends on $\boldsymbol{x}$ through the phase r and through $\boldsymbol{\sigma}_n(\boldsymbol{x})$ and $p_n(\boldsymbol{x})$. The comparison potential $\mathcal{D}_0$ is chosen as

$$\begin{aligned}\mathcal{D}_0\left(\dot{\boldsymbol{\varepsilon}}, \dot{\boldsymbol{\varepsilon}}^{\mathsf{p}}, \dot{p}\right) &= \frac{\Delta t}{2}\left[(\dot{\boldsymbol{\varepsilon}} - \dot{\boldsymbol{\varepsilon}}^{\mathsf{p}}) : \boldsymbol{L}_0^{(r)} : (\dot{\boldsymbol{\varepsilon}} - \dot{\boldsymbol{\varepsilon}}^{\mathsf{p}})\right] + \boldsymbol{\sigma}_n^{(r)} : (\dot{\boldsymbol{\varepsilon}} - \dot{\boldsymbol{\varepsilon}}^{\mathsf{p}}) \\ &+ \frac{1}{\Delta t}\left(w_{st}^{(r)}(p_n + \Delta t\dot{p}) - w_{st}^{(r)}(p_n)\right) \\ &+ \frac{\eta^{(r)}\dot{\varepsilon}_0}{m+1}\left(\frac{\dot{p}}{\dot{\varepsilon}_0}\right)^{m+1} + I_{\{\dot{p} = \dot{\varepsilon}^{\mathsf{p}}_{\mathsf{eq}}\}}(\dot{\boldsymbol{\alpha}}) + \eta_0^{(r)}\dot{\boldsymbol{\varepsilon}}^{\mathsf{p}} : \dot{\boldsymbol{\varepsilon}}^{\mathsf{p}}.\end{aligned}$$

It is found in the different optimization steps involved in the right-hand-side of (18) that, in the comparison composite, $\dot{p}$ is uniform per phase and given as

$$\dot{p} = \dot{p}^{(r)} = \sqrt{\left\langle \frac{2}{3}\dot{\varepsilon}^{\mathsf{p}} : \dot{\varepsilon}^{\mathsf{p}} \right\rangle^{(r)}}.$$

By integration in time, p itself is uniform per phase, $p = p^{(r)}$ in phase r. Note also that the field $\boldsymbol{\sigma}_n(\boldsymbol{x})$ appearing in $\mathcal{D}$ has been replaced in $\mathcal{D}_0$ by a stress $\boldsymbol{\sigma}_n^{(r)}$ which is uniform on phase r . Therefore $\mathcal{D}_0$ is uniform in each individual phase as a function of $\dot{\boldsymbol{\varepsilon}}$ and $\dot{\boldsymbol{\alpha}}$. The conditions for the optimal choice of the variables $\boldsymbol{L}_0^{(r)}$, $\boldsymbol{\sigma}_n^{(r)}$ and $\eta_0^{(r)}$ can be expressed as conditions on the first and second moments per phase of the stress field $\boldsymbol{\sigma}(\boldsymbol{x})$ in the comparison composite. From now on, $\boldsymbol{\sigma}$ denotes the stress field in the comparison composite, solution of the variational problem (20) defining $\widetilde{d}_0$. Setting

$$\widehat{\boldsymbol{\sigma}}_n(\boldsymbol{x}) = \mathcal{H}^{(r)}\boldsymbol{\sigma}(\boldsymbol{x}) + (\boldsymbol{I} - \mathcal{H}^{(r)}) : \boldsymbol{\sigma}_n^{(r)}, \quad \mathcal{H}^{(r)} = \boldsymbol{I} - \boldsymbol{L}^{(r)} : (\boldsymbol{L}_0^{(r)})^{-1},$$

the optimality conditions for $\boldsymbol{L}_0^{(r)}$ and $\boldsymbol{\sigma}_n^{(r)}$ read as (Lahellec and Suquet [27]):

$$\langle \boldsymbol{\sigma}_n \rangle^{(r)} = \langle \hat{\boldsymbol{\sigma}}_n \rangle^{(r)} \quad \text{and} \quad \langle \boldsymbol{\sigma}_n \otimes \boldsymbol{\sigma}_n \rangle^{(r)} = \langle \widehat{\boldsymbol{\sigma}}_n \otimes \widehat{\boldsymbol{\sigma}}_n \rangle^{(r)}, \tag{21}$$

whereas the optimality with respect to $\eta_0^{(r)}$ yields:

$$\eta_0^{(r)} = \frac{1}{3}\frac{\overline{\overline{\sigma}}_{\mathsf{eq}}^{(r)}}{\dot{\varepsilon}_0}\left(\frac{\eta^{(r)}}{\left[\overline{\overline{\sigma}}_{\mathsf{eq}}^{(r)} - \sigma_Y^{(r)} - R^{(r)}(p^{(r)})\right]^+}\right)^{n^{(r)}}. \tag{22}$$

Equations (21) and (22) define a nonlinear problem for $\boldsymbol{L}_0^{(r)}$, $\boldsymbol{\sigma}_n^{(r)}$ and $\eta_0^{(r)}$ since the first and second moments of $\boldsymbol{\sigma}$ depend on these unknowns which, themselves, depend on these first and second moments of $\boldsymbol{\sigma}$.

3.5 Interpretation of the LCC

The constitutive relations of the phases in the LCC (deduced from the above expression of $\mathcal{D}_0$) can be written as

$$\dot{\boldsymbol{\varepsilon}} = \boldsymbol{M}_0^{(r)} : \left(\frac{\boldsymbol{\sigma} - \boldsymbol{\sigma}_n^{(r)}}{\Delta t} \right) + \frac{1}{2\eta_0^{(r)}} \boldsymbol{s}, \tag{23}$$

where $\eta_0^{(r)}$ is given by (22). The relations (23) between $\dot{\boldsymbol{\varepsilon}}$ and $\boldsymbol{\sigma}$ are that of a "thermoelastic" composite with compliance $\boldsymbol{M}^{(r)} = 1/\Delta t \boldsymbol{M}_0^{(r)} + 1/2\eta_0^{(r)} \boldsymbol{K}$ ($\boldsymbol{K}$ is the 4th-order projector on deviators) and "thermal" eigenstrain $-1/\Delta t \boldsymbol{M}_0^{(r)} : \boldsymbol{\sigma}_n^{(r)}$. They are the time-discretized version of a linear viscoelastic composite (different from one time-step to the other). The comparison composite is therefore a *linear* comparison composite which can be seen either as a viscoelastic composite (in a time continuous interpretation of (23)) or as a thermoelastic composite (in a time-discretized interpretation).

The constitutive relations (23) can alternatively be put in the form:

$$\left.\begin{aligned} \dot{\boldsymbol{\varepsilon}} &= \boldsymbol{M}_0^{(r)} : \left(\frac{\boldsymbol{\sigma} - \boldsymbol{\sigma}_n^{(r)}}{\Delta t} \right) + \dot{\boldsymbol{\varepsilon}}^{\mathsf{p}}, \quad \dot{\boldsymbol{\varepsilon}}^{\mathsf{p}} = \frac{3}{2} \dot{p}^{(r)} \frac{\boldsymbol{s}}{\overline{\overline{\sigma}}_{\mathsf{eq}}^{(r)}}, \\ \dot{p}^{(r)} &= \dot{\varepsilon}_0 \left(\frac{\left[\overline{\overline{\sigma}}_{\mathsf{eq}}^{(r)} - \sigma_Y^{(r)} - R^{(r)}(p^{(r)}) \right]^+}{\eta^{(r)}} \right)^{n^{(r)}} . \end{aligned}\right\} \tag{24}$$

Interestingly, these equations have the same structure as the initial constitutive relations but are *nonlocal* in the sense that the driving force for the plastic deformation $\boldsymbol{\varepsilon}^{\mathsf{p}}(\boldsymbol{x})$ *is not the local stress* $\boldsymbol{\sigma}(\boldsymbol{x})$ at point $\boldsymbol{x}$ but is *the second moment of the stress field over phase* r (or more specifically its second invariant $\overline{\overline{\sigma}}_{\mathsf{eq}}^{(r)}$). It should be noted that (22) defines $\eta_0^{(r)}$ as a *secant* viscosity for the purely viscous problem. Therefore the present method can be interpreted as follows:

- The nonlinear constitutive equations are linearized (using a secant method) to obtain a linear viscoelastic comparison composite (LCC),
- The elastic moduli of the LCC differ from that of the original composite and a piecewise uniform stress is substituted to the spatially varying stress field at the beginning of the time step in order to integrate

accurately in time the evolution of the linear viscoelastic comparison composite,

- The choice of this comparison composite is made according to the Rate-Variational Principle (20) leading, for an isotropic elasto-(visco)plastic phase governed by the constitutive relations (1), to the optimality conditions (21) and (22).

3.6 Elasto-(visco)plastic polycrystals

The constitutive equations (2) cannot be put, strictly speaking, in the form (9) for generalized standard materials. However, the above described procedure for defining a linear comparison composite can be followed (without the justification of a variational principle) with the additional flexibility of choosing a different linearization procedure. After several trial and errors, we came to the conclusion that the best compromise for this linearization of the constitutive equations (2) is the more advanced second-order method of Liu and Ponte Castañeda [29] to linearize the evolution equation for $\dot{\gamma}_k$ and more standard first or second moment equations for the other evolution equations. The constitutive relations for single crystals in the LCC are taken as:

$$\left.\begin{array}{c}
\dot{\boldsymbol{\varepsilon}}(\boldsymbol{x}) = \boldsymbol{M}_0{}^{(r)} : \left(\dfrac{\boldsymbol{\sigma}(\boldsymbol{x}) - \boldsymbol{\sigma}_n^{(r)}}{\Delta t} \right) + \boldsymbol{\delta\varepsilon}^{\mathsf{vp}}(\boldsymbol{x}), \\
\boldsymbol{\delta\varepsilon}^{\mathsf{vp}}(\boldsymbol{x}) = \displaystyle\sum_{k=1}^{M} \delta\gamma_k^{(r)}(\boldsymbol{x}) \boldsymbol{\mu}_k^{(r)}, \\
\delta\gamma_k^{(r)}(\boldsymbol{x}) = \alpha_k^{(r)} (\tau_k^{(r)}(\boldsymbol{x}) - X_k^{(r)}(\boldsymbol{x})) + \beta_k^{(r)}, \\
\delta\tau_{0,k}^{(r)} = \left(\tau_{k,sta} - \tau_{0,k}^{(r)} \right) \delta p_k^{(r)}, \quad \delta p_k^{(r)} = \displaystyle\sum_{\ell=1}^{M} h_{k,\ell}^{(r)} \sqrt{\left\langle \Delta\gamma_\ell^{(r)2} \right\rangle^{(r)}}, \\
\delta X_k^{(r)}(\boldsymbol{x}) = \left(c_k - d_k \left\langle X_k^{(r)} \right\rangle^{(r)} \mathrm{sgn}\delta\gamma_k^{(r)}(\boldsymbol{x}) \right) \delta\gamma_k^{(r)}(\boldsymbol{x}) - \\
\left(d_k \left| \left\langle \delta\gamma_k^{(r)} \right\rangle^{(r)} \right| + e_k \right) X_k(\boldsymbol{x}) + d_k \left| \left\langle \delta\gamma_k^{(r)} \right\rangle^{(r)} \right| \left\langle X_k^{(r)} \right\rangle^{(r)}.
\end{array}\right\} \tag{25}$$

where

$$\delta\gamma_k^{(r)}(\boldsymbol{x}) = \frac{\gamma_k^{(r)}(\boldsymbol{x}) - \gamma_{k,n}^{(r)}}{\Delta t}, \quad \delta X_k^{(r)}(\boldsymbol{x}) = \frac{X_k^{(r)}(\boldsymbol{x}) - \left\langle X_{k,n}^{(r)} \right\rangle^{(r)}}{\Delta t}, \quad \delta\tau_{0,k}^{(r)} = \frac{\tau_{0,k}^{(r)} - \tau_{0,k,n}^{(r)}}{\Delta t},$$

and $\alpha_k^{(r)}$ and $\beta_k^{(r)}$ solve the nonlinear equations

$$\beta_k^{(r)} = f_k(\bar{\iota}_k^{(r)}) - \alpha_k^{(r)}\bar{\iota}_k^{(r)}, \quad \alpha_k^{(r)} = \frac{f(\hat{\iota}_k^{(r)}) - f(\bar{\iota}_k^{(r)})}{\hat{\iota}_k^{(r)} - \bar{\iota}_k^{(r)}}, \quad f_k(\iota) = \dot{\gamma}_{0,k}\left(\frac{|\iota|}{\tau_{0,k}}\right)^{n_k-1}\iota,$$

where

$$\iota_k^{(r)}(\boldsymbol{x}) = \tau_k^{(r)}(\boldsymbol{x}) - X_k^{(r)}(\boldsymbol{x}), \quad \bar{\iota}_k^{(r)} = \left\langle \iota_k^{(r)} \right\rangle^{(r)}, \quad \hat{\iota}_k^{(r)} = \bar{\iota}_k^{(r)} + \sqrt{\left\langle {\iota_k^{(r)}}^2 \right\rangle^{(r)}}.$$

${\boldsymbol{M}_0}^{(r)}$ and $\boldsymbol{\sigma}_n^{(r)}$ are determined by imposing closure equations similar to (21).

4 Sample results

4.1 Effective transient response

The model based on the Rate-Variational Principle will be called the RVP model. It can now be applied to the two specific problems described in the introduction.

4.1.1 Bauschinger effect in dual-phase steels

The predictions of the RVP model are compared with the full-field simulations of Brassart *et al* [11] for the specific case of dual-phase steels composed of a ferritic soft matrix containing hard martensitic inclusions. The inclusions (phase 1) are purely elastic ($E^{(1)} = 200$ GPa, $\nu^{(1)} = 0.3$), the matrix (phase 2) is a rate-independent material with isotropic hardening and the following characteristics:

$$E^{(2)} = 200 \text{ GPa}, \ \nu^{(2)} = 0.3,$$

$$\sigma_{\mathsf{eq}} = \sigma_Y^{(2)} + \beta p^{\gamma}, \ \sigma_Y^{(2)} = 300 \text{ MPa}, \ \beta^{(2)} = 1130 \ \text{ MPa}, \ \gamma^{(2)} = 0.31.$$

The Hashin-Shtrikman lower bound is used to estimate the effective properties of the LCC. The RVP model predicts rather accurately the early yielding in compression of the composite and the rather long transition zone between elastic unloading and fully developed plasticity in compression (see figure 3 left).

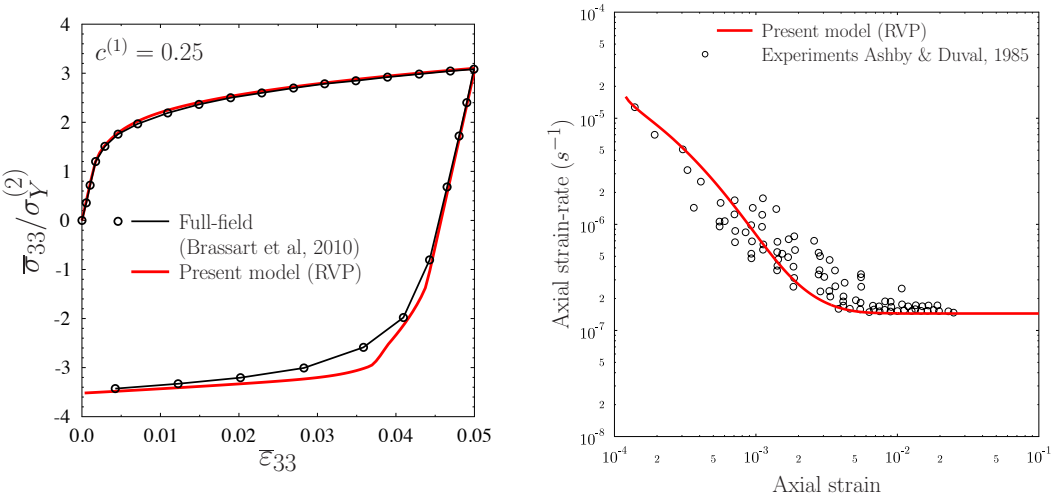

Figure 3: Left: Dual-phase steel, comparison between the full field simulations of Brassart [11] and the RVP model. Right: transient creep of polycrystalline ice, comparison between experimental results compiled by Ashby and Duval [13] and the RVP model.

4.1.2 Transient creep in polycrystals

The RVP model (25) has been applied to polycrystalline ice under creep and its prediction can be compared to the experimental results compiled by Ashby and Duval [13]. Material data for the single crystal model (2) are given in Suquet *et al* [15]. The effective properties of the LCC are estimated by the self-consistent scheme. As can be seen in figure 3 right, the predictions of the RVP model are in good agreement with the experimental results.

4.2 Field statistics

The RVP model not only delivers the effective response of the composite but gives also access to the field statistics in the LCC which can be considered as an approximation of the field statistics in the actual nonlinear composite.

4.2.1 Two-phase system. Rate-dependent matrix

Full-field simulations have been performed to simulate the effective response, as well as the local response, of a two-phase composite comprised of a rate-dependent matrix containing elastic inclusions with volume fraction $c^{(1)} = 0.17$. Fifty spherical inclusions are arranged randomly in a cubic unit-cell and a FFT technique (Moulinec and Suquet [30]) is used to simulate the response of the unit-cell to a loading-unloading test under a prescribed history of macroscopic strain (see Lahellec and Suquet [27] for details):

$$\overline{\boldsymbol{\varepsilon}}(t) = \varepsilon_{33}(t)\left(-\frac{1}{2}\boldsymbol{e}_1\otimes\boldsymbol{e}_1 - \frac{1}{2}\boldsymbol{e}_2\otimes\boldsymbol{e}_2 + \boldsymbol{e}_3\otimes\boldsymbol{e}_3\right), \quad \dot{\varepsilon}_{33}(t) = \pm 6.10^{-2}\ \mathrm{s}^{-1}$$

The inclusions (phase 1) are elastic (with bulk modulus $k^{(1)} = 20$ GPa and shear modulus $\mu^{(1)} = 6$ GPa). The matrix (phase 2) is a rate-dependent material modeled with the constitutive relations (1) with neither isotropic nor kinematic hardening and with the following material characteristics:

$$k^{(2)} = 10 \text{ GPa}, \quad \mu^{(2)} = 3 \text{ GPa},$$

$$\sigma_Y^{(2)} = 100 \text{ MPa}, \quad \eta^{(2)} = 100 \text{ MPa}, \quad \dot{\varepsilon}_0^{(2)} = 1.\ \mathrm{s}^{-1}, \quad n^{(2)} = 3.333.$$

The predictions of the RVP model are compared to full-field simulations. As can be seen in figure 4 (upper center), the overall response of the composite is well predicted by the model.

First and second moments of the stress field in the matrix and in the inclusions are also in good agreement. There is a 30% discrepancy on the stress fluctuations in the matrix, but regarding the rather local character of this quantity, the agreement is satisfactory.

4.2.2 Two-dimensional nonlinear polycrystals under anti-plane shear

The statistics of the fields in the model problem of two-dimensional polycrystals under anti-plane shear has been investigated both by full-field simulations and by the RVP model (25). At the single crystal level, slip can occur along two orthogonal slip systems

$$\boldsymbol{\mu}_1 = \frac{1}{2}(\boldsymbol{e}_1 \otimes \boldsymbol{e}_3 + \boldsymbol{e}_3 \otimes \boldsymbol{e}_1), \quad \boldsymbol{\mu}_2 = \frac{1}{2}(\boldsymbol{e}_2 \otimes \boldsymbol{e}_3 + \boldsymbol{e}_3 \otimes \boldsymbol{e}_2).$$

The in-plane orientation of grain r is denoted by $\omega^{(r)}$. The two initial elastic anti-plane shear moduli are equal ($G_1 = G_2 = 1$ MPa). No hardening (neither isotropic nor kinematic) is taken into account and the slip on the individual slip systems are governed by a pure power-law relation

$$\dot{\gamma}_k = \dot{\gamma}_{0,k} \left(\frac{|\tau_k|}{\tau_{0,k}} \right)^{n_k - 1} \tau_k,$$

$$\gamma_{0,1} = \gamma_{0,2} = 1.0 \text{ s}^{-1}, \quad n_1 = n_2 = 3, \quad \tau_{0,1} = 1.0 \text{ MPa}, \quad \tau_{0,2} = 3.0 \text{ MPa}.$$

The polycrystal is loaded in shear at constant strain-rate:

$$\overline{\boldsymbol{\varepsilon}}(t) = \frac{\dot{\varepsilon}_0 t}{2}(\boldsymbol{e}_1 \otimes \boldsymbol{e}_3 + \boldsymbol{e}_3 \otimes \boldsymbol{e}_1).$$

The effective response and the field fluctuations predicted by the RVP model are compared in figure 5 with full-field simulations. In order to attain stationarity of the field fluctuations, several configurations have to be considered (or the size of the volume element has to be increased). In our case full-field simulations were performed on 8 different configurations corresponding to 8 different Voronoi tessellations. Ensemble averages were performed on the different configurations according to

$$< f >= \frac{1}{N_c} \sum_{j=1}^{N_c} \langle f \rangle^j, \quad \text{with } \langle f \rangle^j \text{ the average of } f \text{ over the } j\text{-th configuration.} \tag{26}$$

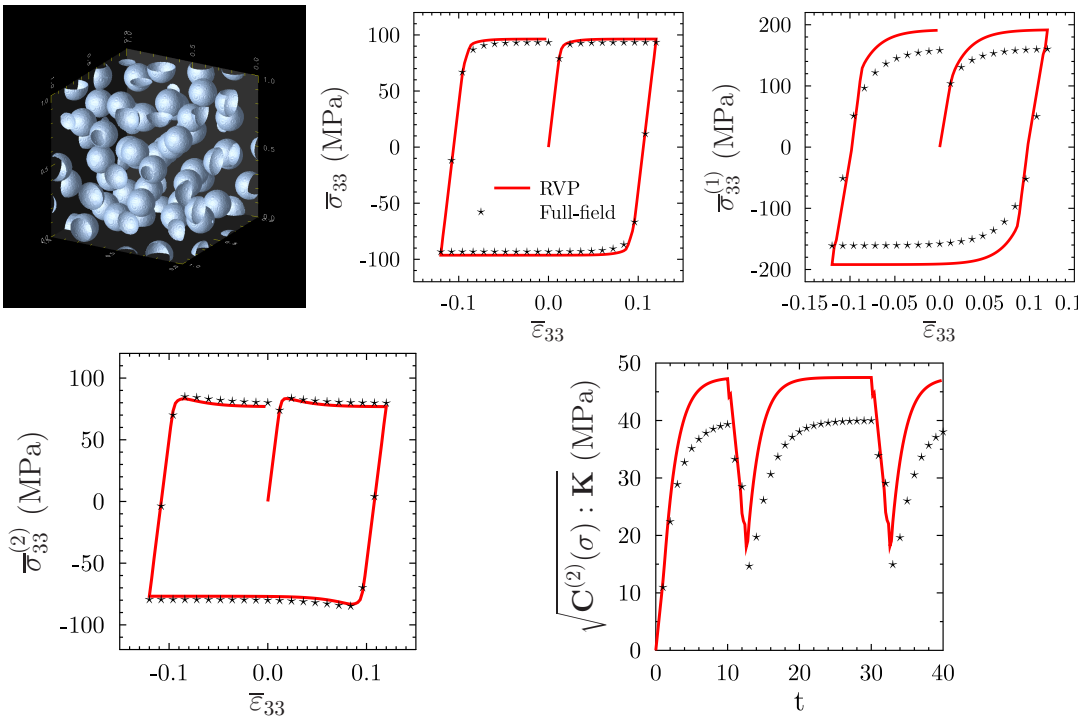

Figure 4: Two-phase system with a rate-dependent matrix. Loading-unloading test. RVP model (solid line) compared with full-field simulations (symbols $\star$). Upper left: configuration used in the FFT full-field simulations (volume fraction of inclusions $c^{(1)} = 0.17$). Upper center: effective response of the composite. Upper right: average stress in the inclusions. Lower left: average stress in the matrix. Lower right: stress fluctuations in the matrix.

The full-field results of the different grains in the different configurations were grouped by angular sectors. Ten different angular sectors were defined (between 0 and π) and the value of a function f over the I-th angular sector was defined as:

$$\langle f \rangle^I = \frac{1}{N_c} \sum_{j=1}^{N_c} \sum_i \frac{c^{(i)}}{c^I} \langle f \rangle_i^j \quad \text{and} \quad \left\langle f^2 \right\rangle^I = \frac{1}{N_c} \sum_{j=1}^{N_c} \sum_i \frac{c^{(i)}}{c^I} \left\langle f^2 \right\rangle_i^j \tag{27}$$

with $c^I = \sum_i c^{(i)}$), for grains with orientation $\omega^{(i)}$ such that $\frac{\pi(I-1)}{10} \leq \omega^{(i)} < \frac{\pi I}{10}$ and $I = 1, ..., 10$. The stress fluctuations as a function of the angular sector are defined in a similar way as:

$$\boldsymbol{C}^I(\boldsymbol{\sigma}) :: \boldsymbol{K} = 2 \left\langle \left(\sigma_{13} - \langle \sigma_{13} \rangle_I\right)^2 + \left(\sigma_{23} - \langle \sigma_{23} \rangle_I\right)^2 \right\rangle_I$$

The stress fluctuations are shown at three different times t_1, t_2 and t_3 corresponding to the initial elastic response, the transient response and the fully viscous response of the polycrystal as a function of the grain orientation. There is initially no stress fluctuation at time t_1 since the two elastic shear moduli are equal (the single crystal is elastically isotropic and the polycrystal is elastically homogeneous). Then stress fluctuations begin to develop in the transient regime (time t_2) and culminate in the purely viscous regime where the properties of the phases are contrasted. As can be seen, the RVP model captures correctly the dependence of the stress fluctuations both as a function of time t and orientation ω.

5 Concluding remarks

A variational approach to the effective response of elasto-plastic heterogeneous materials with isotropic and kinematic hardening has been proposed. Central to this approach is an incremental variational principle satisfied by the rate of internal variables in single phases governed by two potentials. Then, inspired by the variational method of Ponte Castañeda, the original potential is compared with a reference potential for a linear comparison composite for which the variational problem can be solved in closed form. Appropriate choices for the reference potential lead to approximate models for the exact effective potential. The effective response of the composite as

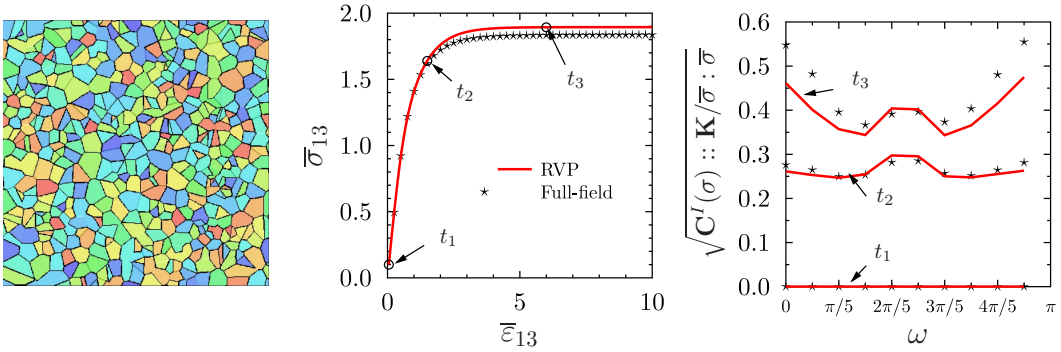

Figure 5: Two-dimensional polycrystals under anti-plane shear. Monotonic loading at constant strain-rate. RVP model (solid line) compared with full-field simulations (symbols $\star$)). Left: one of the configurations used in the FFT full-field simulations. Center: effective response (the full-field simulations correspond to the ensemble average over all configurations). Right: stress fluctuations as a function of the orientation.

well as the first and second moments of the stress field in the phases are accurately described. In particular the Bauschinger effect commonly observed in metal-matrix composites is captured by the method.

Acknowledgments This study was partly funded by the French 'Agence Nationale de la Recherche' (project ELVIS, #ANR-08-BLAN-0138).

References

[1] M. Uchic, M. Groeber, D. Dimiduk, J. Simmons, 3D microstructural characterization of nickel superalloys via serial-sectioning using a dual beam FIB-SEM, Scripta Materialia **55** (2006) 23–28.

[2] P. Ponte Castañeda, P. Suquet, Nonlinear composites, in: E. V. der Giessen, T. Wu (Eds.), Advances in Applied Mechanics, Vol. **34**, Academic Press, New York, 1998, pp. 171–302.

[3] R. Lebensohn, A. Rollett, P. Suquet, Fast Fourier Transform-based modelling for the determination of micromechanical fields in polycrystals, Journal of Materials **63** (2011) 13–18.

[4] J. Willis, The structure of overall constitutive relations for a class of nonlinear composites, IMA J. Appl. Math. **43** (1989) 231–242.

[5] P. Ponte Castañeda, The effective mechanical properties of nonlinear isotropic composites, J. Mech. Phys. Solids **39** (1991) 45–71.

[6] P. Doumalin, M. Bornert, J. Crépin, Characterisation of the strain distribution in heterogeneous materials, Mécanique & Industries **4** (2003) 607–617.

[7] M. Bourcier, A. Dimanov, E. Héripré, J. Raphanel, M. Bornert, G. Desbois, Full field investigation of salt deformation at room temperature: cooperation of crystal plasticity and grain sliding, in: B. T. F.P.J. Rimrott (Ed.), Mechanical Behavior of Salt VII, Balkema/Taylor & Francis, 2012, pp. 37–43.

[8] P. Ponte Castañeda, Second-order homogenization estimates for nonlinear composites incorporating field fluctuations. I - Theory., J. Mech. Phys. Solids **50** (2002) 737–757.

[9] N. Lahellec, P. Suquet, Effective behavior of linear viscoelastic composites: a time-integration approach, Int. J. Sol. Struct. **44** (2007) 507–529.

[10] S. Corbin, D. Wilkinson, J. Embury, The Bauschinger effect in a particulate reinforced Al alloy, Materials Science and Engineering **A 207** (1996) 1–11.

[11] L. Brassart, I. Doghri, L. Delannay, Homogenization of elasto-plastic composites coupled with a nonlinear finite element analysis of the equivalent inclusion problem, Int. J. Solids Struct. **47** (2010) 716–729.

[12] I. Doghri, L. Brassart, L. Adam, J. Gérard, A second-moment incremental formulation for the mean-field homogenization of elasto-plastic composites, Int. J. Plasticity **27** (2011) 352–371.

[13] M. Ashby, P. Duval, The creep of polycrystalline ice, Cold Reg. Sci. Technol. 11 (1985) 285–300.

[14] O. Castelnau, P. Duval, M. Montagnat, R. Brenner, Elastoviscoplastic micromechanical modeling of the transient creep of ice, J. Geophysical Research 113 (2008) B11203.

[15] P. Suquet, H. Moulinec, O. Castelnau, N. Lahellec, M. Montagnat, F. Grennerat, P. Duval, R. Brenner, Multi-scale modeling of the mechanical behavior of polycrystalline ice under transient creep, Procedia IUTAM **3** (2012) 76–90.

[16] P. Ponte Castañeda, Exact second-order estimates for the effective mechanical properties of nonlinear composite materials, J. Mech. Phys. Solids **44** (1996) 827–862.

[17] J. Eshelby, The determination of the elastic field of an ellipsoidal inclusion and related problems, Proc. R. Soc. London A **241** (1957) 376–396.

[18] Z. Hashin, Analysis of Composite Materials: A survey, J. Appl. Mech. **50** (1983) 481–503.

[19] V. Buryachenko, Multiparticle effective field and related methods in micromechanics of composite materials, Appl. Mech. Rev. 54 (2001) 1–47.

[20] M. Idiart, P. Ponte Castañeda, Field statistics in nonlinear composites. I. Theory., Proc. R. Soc. A **463** (2007) 183–202.

[21] N. Lahellec, P. Ponte Castañeda, P. Suquet, Variational estimates for the effective response and field statistics in thermoelastic composites with intra-phase property fluctuations, Proceedings of the Royal Society A **447** (2011) 2224–2246.

[22] N. Lahellec, P. Suquet, Effective response and field statistics in viscoelastic composites , in preparation.

[23] P. Ponte Castañeda, New variational principles in plasticity and their application to composite materials, J. Mech. Phys. Solids **40** (1992) 1757–1788.

[24] P. Mialon, Eléments d'analyse et de résolution numérique des relations de l'élasto-plasticité., Tech. rep., EDF.Bulletin de la Direction des Etudes et recherches. Série C. Mathématiques, Informatique (1986).

[25] M. Ortiz, E. Repetto, Nonconvex energy minimization and dislocation structures in ductile single crystals, J. Mech. Phys. Solids **47** (1999) 397–462.

[26] C. Miehe, J. Schotte, M. Lambrecht, Homogenization of inelastic materials at finite strains based on incremental variational principles. Application to the texture analysis of polycrystals., J. Mech. Phys. Solids **50** (2002) 2123–2167.

[27] N. Lahellec, P. Suquet, Effective response and field statistics in elasto-viscoplastic and elasto-plastic composites under radial and non-radial loadings , submitted.

[28] N. Lahellec, P. Suquet, On the effective behavior of nonlinear inelastic composites: I. Incremental variational principles, J. Mech. Phys. Solids **55** (2007) 1932–1963.

[29] Y. Liu, P. Ponte Castañeda, Second-order theory for the effective behavior and field fluctuations in viscoplastic polycrystals, J. Mech. Phys. Solids **52** (2004) 467–495.

[30] H. Moulinec, P. Suquet, A numerical method for computing the overall response of nonlinear composites with complex microstructure, Comp. Meth. Appl. Mech. Engng. **157** (1998) 69–94.